The Plant Cell, Vol. 12, 2409–2423, December 2000, www.plantcell.org © 2000 American Society of Plant Physiologists

PROCUSTE1 Encodes a Cellulose Synthase Required for Normal Cell Elongation Specifically in Roots and Dark-Grown Hypocotyls of Arabidopsis

Mathilde Fagard,[a,1] Thierry Desnos,[a,2] Thierry Desprez,[a] Florence Goubet,[a,3] Guislaine Refregier,[a] Gregory Mouille,[a] Maureen McCann,[b] Catherine Rayon,[a,4] Samantha Vernhettes,[a] and Herman Höfte[a,5]

[a] Laboratoire de Biologie Cellulaire, Institut National de la Recherche Agronomique, 78026 Versailles Cedex, France
[b] Department of Cell Biology, John Innes Centre, Norwich Research Park, Norwich NR4 7UH, United Kingdom

Mutants at the *PROCUSTE1* (*PRC1*) locus show decreased cell elongation, specifically in roots and dark-grown hypocotyls. Cell elongation defects are correlated with a cellulose deficiency and the presence of gapped walls. Map-based cloning of *PRC1* reveals that it encodes a member (*CesA6*) of the cellulose synthase catalytic subunit family, of which at least nine other members exist in Arabidopsis. Mutations in another family member, *RSW1* (*CesA1*), cause similar cell wall defects in all cell types, including those in hypocotyls and roots, suggesting that cellulose synthesis in these organs requires the coordinated expression of at least two distinct cellulose synthase isoforms.

INTRODUCTION

Cellulose, the most abundant biopolymer, is produced by plants, bacteria, and certain animal species; it consists of simple linear (1→4)-β–linked glucan chains assembled in parallel arrays in semicrystalline microfibrils (Delmer, 1999). In primary walls of most cotyledonous species, cellulose microfibrils constitute an extensible network cross-linked by hydrogen-bonded xyloglucans embedded in a hydrophilic pectin matrix (Carpita and Gibeaut, 1993; McCann and Roberts, 1994). In growing cells, cellulose microfibrils are deposited transversely to the elongation axis and are thus thought to constrain growth in one direction. Cortical microtubule arrays often parallel the orientation of the microfibrils and appear to play a key role in controlling the orientation of the microfibrils in the primary wall (Giddings and Staehelin, 1991; Wymer and Lloyd, 1996). Not only do microfibrils control cell shape, but also their orientation in meristematic tissues controls the formation of organ primordia (Green, 1994) and thus plays a key role in the control of plant architecture.

When cell expansion is arrested, a secondary wall is deposited within the bounds of the primary wall. The matrix polysaccharide composition of the secondary wall differs from that of the primary wall and frequently contains a high proportion of lignin. In addition, microfibrils are mostly deposited in the secondary wall in helical arrays in successive layers of alternating pitch (Vian and Reis, 1991). As a result, this wall is much more rigid and provides strength and resistance against compressive forces, in contrast to the flexible primary walls of organs, which maintain their shape as a result of turgor pressure within their tissues. In summary, these observations show that a thorough understanding of the molecular mechanism and the regulation of cellulose synthesis is indispensable for understanding multiple aspects of plant development.

To date, cellulose synthesis remains poorly understood (Kawagoe and Delmer, 1997; Delmer, 1999). UDP-glucose is the direct substrate added to the nonreducing end of the growing (1→4)-β-glucan chain. In plants, a membrane-bound sucrose synthase, the enzyme that converts sucrose to UDP-glucose, may be linked physically to the cellulose synthase complex and may play an important role in channeling sucrose into the cellulose synthase complex (Amor et al., 1995). The biochemistry of cellulose synthesis is extremely complex, and thus far no efficient procedure to assay this activity in vitro has been described (Delmer, 1999). In contrast to other cell wall polysaccharides, which are synthesized in the Golgi apparatus and transported to the cell surface by vesicles, cellulose is thought to be synthesized by plasma membrane–bound complexes. These complexes, which can be visualized in higher plants as hexameric

[1] Current address: Friedrich Miescher Institut, P.O. Box 2543, 4002 Basel, Switzerland.
[2] Current address: Département d'Ecophysiologie Végétale et de Microbiologie/Laboratoire du Métabolisme Carboné, Commissariat à l'Energie Atomique de Cadarache, 13108 St. Paul-lez-Durance Cedex, France.
[3] Current address: Department of Biochemistry, University of Cambridge, Cambridge CB2 1QW, UK.
[4] Current address: Department of Botany and Plant Pathology, Purdue University, West Lafayette, IN 47907-1155.
[5] To whom correspondence should be addressed. E-mail hofte@versailles.inra.fr; fax 33-1-30-83-30-99.

clusters of particles on freeze-fractured plasma membranes, have been named rosette terminal complexes (TCs) or simply rosettes (Emons, 1985).

Genes encoding homologs of the catalytic subunit of cellulose synthase in bacteria have been identified in higher plants (Pear et al., 1996). The roles of at least two family members (*CesA1* and *CesA7*) in the synthesis of cellulose were further demonstrated by the identification of mutants in Arabidopsis. *rsw1* carries a mutation in *CesA1* that causes a temperature-sensitive radial cell expansion defect and a cellulose deficiency in all cell types investigated (Arioli et al., 1998). In this mutant, moreover, the TCs disappear on images of freeze-fractured plasma membranes. *irx3* is mutated in *CesA7* and shows a collapsed xylem phenotype and a greatly decreased cellulose content specifically in secondary cell walls (Taylor et al., 1999). These genes thus appear to encode functionally specialized isoforms required for cellulose synthesis in primary or secondary walls. Recently, Kimura et al. (1999) showed that antibodies generated against a member of the cellulose synthase catalytic subunit family preferentially labeled TCs in freeze-fractured plasma membranes of *Vigna angularis*; thus, TCs were definitively identified as the site of cellulose synthesis.

Besides the polymerization of (1→4)-β-glucan, the assembly of the newly synthesized polymer into microfibrils remains poorly understood. The analysis of *rsw1* suggested that the synthesis and formation of microfibrils are two independent processes. Indeed, at the restrictive temperature and in the absence of functional rosettes, an ammonium oxalate–soluble, presumably noncrystalline, (1→4)-β-glucan accumulated (Arioli et al., 1998). Similarly, cotton fibers grown in vitro in the presence of the herbicide Novartis CGA 325′615, which also inhibits the formation of rosettes, produced (1→4)-β-glucan, but also produced it in an alkali or ammonium oxalate–extractable form (Delmer, 1999). These observations are consistent with the view that RSW1 and related proteins polymerize (1→4)-β-glucans but mediate crystallization into microfibrils only when they are associated in TCs.

Cellulose synthase catalytic subunits are encoded by a large gene family. In Arabidopsis, at least 10 isoforms are recognized (http://cellwall.stanford.edu/cellwall and http://www-plb.ucdavis.edu/labs/delmer/genes.html). The strong mutant phenotypes for *RSW1* (*CesA1*) and *IRX3* (*CesA7*) suggest a functional specialization for these isoforms. The functions of the other family members remain to be determined. Besides the catalytic subunits, presumably other genes are involved in cellulose synthesis. In the bacteria *Acetobacter xylinum* and *Agrobacterium tumefaciens*, several genes besides the cellulose synthase catalytic subunit are essential for cellulose synthesis, although their exact functions remain to be determined (Saxena et al., 1990; Matthysse et al., 1995a, 1995b). Interestingly, one of the essential genes in Agrobacterium encodes an endo-(1→4)-β-glucanase, which has been proposed to play a controversial role in the cleavage of lipid-linked intermediates of the biosynthetic pathway. In plants, a membrane-bound endo-(1→4)-β-glucanase, KOR, also may play a role in cellulose synthesis, as suggested by the cellulose deficiency of *kor* mutants (Nicol et al., 1998; M. Fagard, G. Mouille, F. Goubet, and H. Höfte, unpublished data).

In this article, further insight is provided regarding the cellulose synthesis machinery of plants. We report the cloning of *PROCUSTE1* (*PRC1*), which was identified previously by mutations causing a growth defect in roots and dark-grown hypocotyls (Desnos et al., 1996). Here, we show that the decreased cell expansion in the dark-grown hypocotyl is correlated with a deficiency in cellulose and the presence of gaps in internal cortical and epidermal cell walls. *PRC1* was cloned and found to encode a novel member of the CesA family, CesA6. Interestingly, both *rsw1* and *prc1* mutants caused a cell elongation defect and cellulose deficiency in roots and dark-grown hypocotyls; however, *prc1* affected only a subset of the cell types that were affected in *rsw1*. This suggests that cellulose synthesis in this subset of cell types requires the coordinated activity of at least two *CesA* isoforms.

RESULTS

Identification of Additional *prc1* Alleles

Fourteen new alleles of the *prc1* locus were identified from Arabidopsis populations mutagenized with ethyl methanesulfonate, T-DNA, or x-rays. Among them were the previously described *quill* (*qui*) mutants (Hauser et al., 1995), which were shown to be allelic to *prc1* (data not shown; see below). *qui1*, *qui2*, and *qui3* were renamed *prc1-9*, *prc1-10*, and *prc1-11*, respectively. Figure 1A shows the hypocotyl lengths of seedlings for nine *prc1* alleles grown for 7 days in complete darkness. Consistent with previous results (Desnos et al., 1996), all alleles (regardless of ecotype) showed a four- to fivefold decrease in hypocotyl length compared with that of wild-type seedlings, whereas no large variations in allele strength were observed (Figure 1A). Root length was also determined for seedlings grown for 7 days in white light on agar medium containing 4.5% sucrose (Figure 1B), conditions under which roots of *qui* alleles exhibit a strong radial expansion phenotype (Hauser et al., 1995). As expected, *prc1* roots were 1.5- to twofold shorter than were wild-type roots, with greater variations between alleles than those observed for dark-grown hypocotyls. On the basis of these root lengths, *prc1-3* and *prc1-4* appeared to be the strongest alleles.

Alterations in Cell Wall Structure in Dark-Grown *prc1* Hypocotyls

The *prc1* phenotype can be phenocopied by treating wild-type seedlings with cellulose biosynthesis inhibitors such as

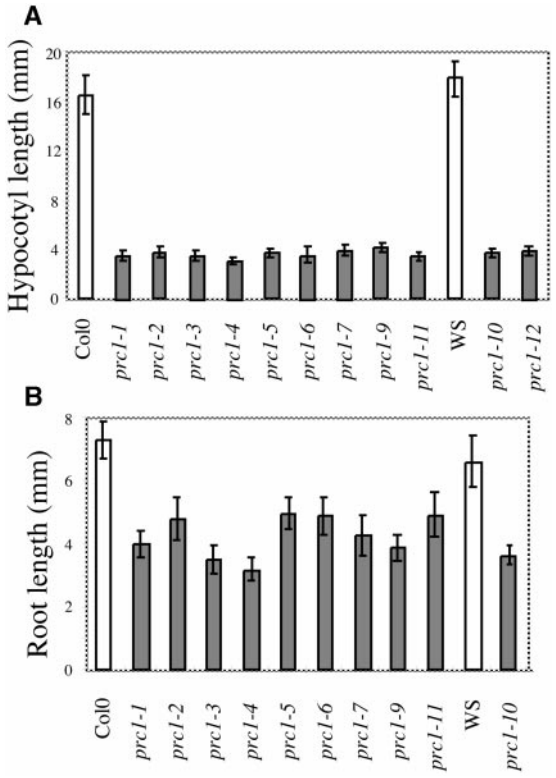

Figure 1. *prc1* Mutants Show Reduced Elongation of Roots and Dark-Grown Hypocotyls.

(A) Dark-grown hypocotyl lengths of wild-type (ecotypes Columbia [Col-0] and Wassilewskija [WS]) seedlings and 11 *prc1* alleles. Seedlings were grown for 7 days in total darkness on sucrose-free agar medium.

(B) Root lengths of wild-type seedlings and 10 *prc1* alleles. Seedlings were grown for 7 days in 16-hr-light/8-hr-dark cycles on agar medium containing 4.5% sucrose.

prc1-1 through *prc1-9* and *prc1-11* are Col-0 alleles; *prc1-10* and *prc1-12* are Ws ecotype.

Error bars indicate ±SD.

2,6-dichlorobenzonitrile (DCB) or isoxaben (data not shown). To look for potential cell wall defects, we studied transverse sections halfway through hypocotyls of 4-day-old dark-grown seedlings after staining with Calcofluor or Congo Red (Figure 2). Calcofluor stains cellulose, callose, and other nonsubstituted or weakly substituted β-glucans (Maeda and Ishida, 1967), whereas Congo Red more generally stains reducing sugars. As shown in Figure 2, no differences in the numbers of cells or tissue layers were observed. However, similar to the DCB-treated seedlings, *prc1-1* hypocotyls were larger than were wild-type hypocotyls, with more radially expanded cells in epidermis, cortex, and endodermis. Interestingly, in almost every cross-section of dark-grown *prc1-1* hypocotyls, incomplete cell walls were found (Figure 2B, top arrow). Incomplete walls were found in epidermal, cortical, and endodermal cell layers. The protruding wall ends were frequently found to be linked by a membranous structure not stained by Calcofluor but observable with Congo Red (Figure 2C) or other stains. This structure presumably corresponds to cell membranes surrounding polysaccharidic material. The study of two other alleles (*prc1-3* and *prc1-7*; data not shown) confirmed the presence of such incomplete cell walls. In some sections (both transverse and longitudinal), cells filled with granular Calcofluor- and Congo Red–stained material were observed (Figure 2B, bottom arrow); these were never observed in the wild type, and the exact nature of the material remains to be determined.

Incomplete cell walls, referred to as "stubs," have been described in various mutants that are defective in cytokinesis (Liu et al., 1995a; Assaad et al., 1996; Lukowitz et al., 1996). Because cortical and most epidermal cells in Arabidopsis hypocotyls have an embryonic origin and do not divide during postembryonic development, we examined sections through *prc1-1* embryos (illustrated for a torpedo-stage embryo in Figure 2D). Cell wall stubs were never observed. The same was true for mature embryos, or even for transverse sections through mature hypocotyls grown in the light (data not shown). Together, these observations indicate that cytokinesis is unaffected in *prc1* and that the observed gapped walls in dark-grown *prc1* hypocotyls arise during cell expansion.

Incomplete walls were also observed in cortical and epidermal walls in dark-grown *prc1-1* hypocotyls by scanning electron microscopy on freeze-fractured material or by transmission electron microscopy, as shown in Figure 3; incomplete walls were observed as frequently as on sections prepared for light microscopy. This finding strongly suggests that the discontinuous walls were present in living tissue and were not artifacts of the sample preparation. Furthermore, transmission electron microscopy revealed the presence of fibrillar material in the wall gaps (Figure 3B).

Mutations at the *PRC1* Locus and Cellulose Deficiency

prc1 cell walls were analyzed by using Fourier transform infrared (FTIR) microspectroscopy. This technique allows rapid analysis of the cell wall composition of areas of the tissue as small as one or a few cells (McCann et al., 1997). FTIR absorption spectra of 4-day-old dark-grown hypocotyls of wild-type and two mutant alleles of *prc1* were collected from a region of ~60 × 40 μm midway along the hypocotyl and avoiding the central stele. The spectra correspond to the absorption in the mid-IR region (between wave numbers 600 and 4000 cm^{-1}) of essentially longitudinal and transverse cell walls of epidermal and cortical cells (two layers of epidermis and four layers of cortex cells), both of which are cell types that are affected by the *prc1* mutations.

The spectra (20 for each condition) were analyzed by principal components (PCs) analysis (Kemsley, 1998), a statistical

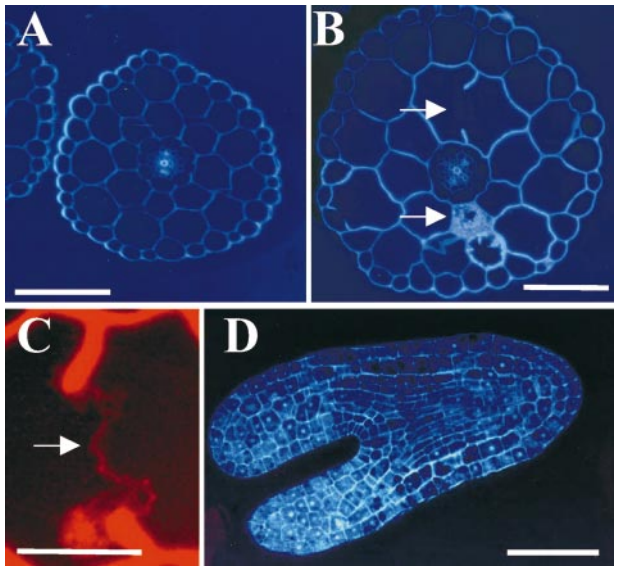

Figure 2. Dark-Grown *prc1* Hypocotyls Contain Incomplete Cell Walls.

(A) and **(B)** Calcofluor-stained hypocotyl cross-sections of 4-day-old dark-grown wild-type **(A)** and *prc1-1* **(B)** seedlings. The top arrow indicates an incomplete wall and the bottom arrow indicates an abnormally filled cell in a *prc1-1* hypocotyl section.

(C) Congo Red–stained section of a *prc1-1* hypocotyl cell in which the incomplete cell wall stubs are connected by a thin structure (arrow).

(D) Calcofluor-stained section through a *prc1-1* immature embryo. No incomplete wall or cell filled with stained material was observed. Bars in **(A)** and **(B)** = 100 μm; bar in **(C)** = 30 μm; bar in **(D)** = 60 μm.

method that reduces the dimensionality of the data from >100 variates (one every 8 cm^{-1} for the region from 1800 to 850 cm^{-1}) to only a few, the PCs. The PCs are ordered in terms of decreasing variance. Each observation (spectrum) has a corresponding set of PC scores describing the variance of that spectrum relative to the mean of the population for each PC. The PC scores of the spectra can then be plotted against one another to reveal patterns or structures in the data (Kemsley, 1998). One can then mathematically derive a "spectrum" (a PC loading) from a PC to identify the molecular factors responsible for the separation of groups of spectra (Kemsley, 1998). As shown in Figure 4A, the analysis showed that wild-type spectra can be separated from *prc1* mutant spectra by using a combination of two PC scores. PC1 explained 72% of the variance. The loading for PC1 (Figure 4B) showed characteristics of purified cellulose in the fingerprint region (peaks at 1038, 1064, 1100, and 1162 cm^{-1}, respectively) and of protein (peaks at 1650 and 1550 cm^{-1}). Peaks at 1650 and 1550 cm^{-1} were negatively correlated with the cellulose fingerprint peaks. Because the PC scores of the spectra of *prc1* seedlings were negative relative to the mean (Figure 4A), the data suggest that the cell walls of *prc1* seedlings are relatively richer in protein and poorer in cellulose than the cell walls of wild-type seedlings. These results show that the changes in *prc1* cell walls are complex but that a major deficiency in crystalline cellulose is a part of the phenotype.

To confirm the observed changes chemically, walls of 4-day-old dark-grown wild-type and *prc1-1* seedlings were isolated and fractionated, and the neutral sugar and uronic acid contents were determined for each fraction. In both wild-type and *prc1-1* seedlings, ~2% of the fresh weight consisted of cell walls. Wall material was extracted consecutively with 0.1 and 4 M KOH, yielding two fractions that were enriched for pectins (fraction 1) and hemicellulose (fraction 2), respectively, as shown by the neutral sugar and uronic acid contents (Figures 5C and 5D). The residual fraction contained 60% glucose (Figure 5E), which indicates an enrichment for cellulose, because as shown below, in the culture conditions used, neither wild-type nor *prc1-1* accumulated significant levels of (1→3)-β-glucan (callose). Also, staining with iodine failed to detect starch in wild-type or *prc1-1* hypocotyls (data not shown). The presence of minor amounts of xylosyl (5%), rhamnosyl (6%), uronic acid (10%), galactosyl (10%), and arabinosyl (6%) residues indicates that a proportion of the noncellulosic polysaccharides also resisted the alkaline treatment, suggesting an intimate association of these polymers with the cellulose microfibrils. Similar observations were reported for cell walls from Arabidopsis leaves (Zablackis et al., 1995).

Strikingly, in mutant walls, the proportions of the three fractions were altered markedly (Figure 5A). Compared with wild-type walls, *prc1-1* walls showed a relative increase in fraction 2, a relative decrease in the residual fraction, and a very minor decrease in fraction 1. Interestingly, in *prc1-1*, the decrease in the residual fraction was not accompanied by a change in the proportions of neutral sugars and uronic acid, suggesting that with less crystalline cellulose present as a substrate, less xyloglucan and pectin resisted the extraction procedure. The neutral sugar and uronic acid contents also remained unchanged for fractions 1 and 2, except for an important decrease of galactosyl residues in fraction 1. This may be the result of a reduction in the number of galactan side chains on the pectins.

To confirm the reduced cellulose production in *prc1*, we measured the incorporation of ^{14}C-glucose into the nitric/acetic acid–insoluble cell wall fraction of actively growing 3-day-old seedlings (Updegraff, 1969). This fraction is 97% (1→4)-β–linked glucose (Peng et al., 2000; data not shown) and is generally considered to be crystalline cellulose. Figure 5B shows that in the wild type, 30% of the label in the cell wall was incorporated in the cellulosic fraction. This proportion was reduced to 17 and 19% in *prc1-1* and *prc1-4*, respectively.

In conclusion, chemical analysis of the cell walls of mutant seedlings confirms the deficiency in cellulose observed by FTIR microspectroscopy. Other changes detected included a relative increase in hemicellulosic polysaccharides and qualitative changes in pectin composition.

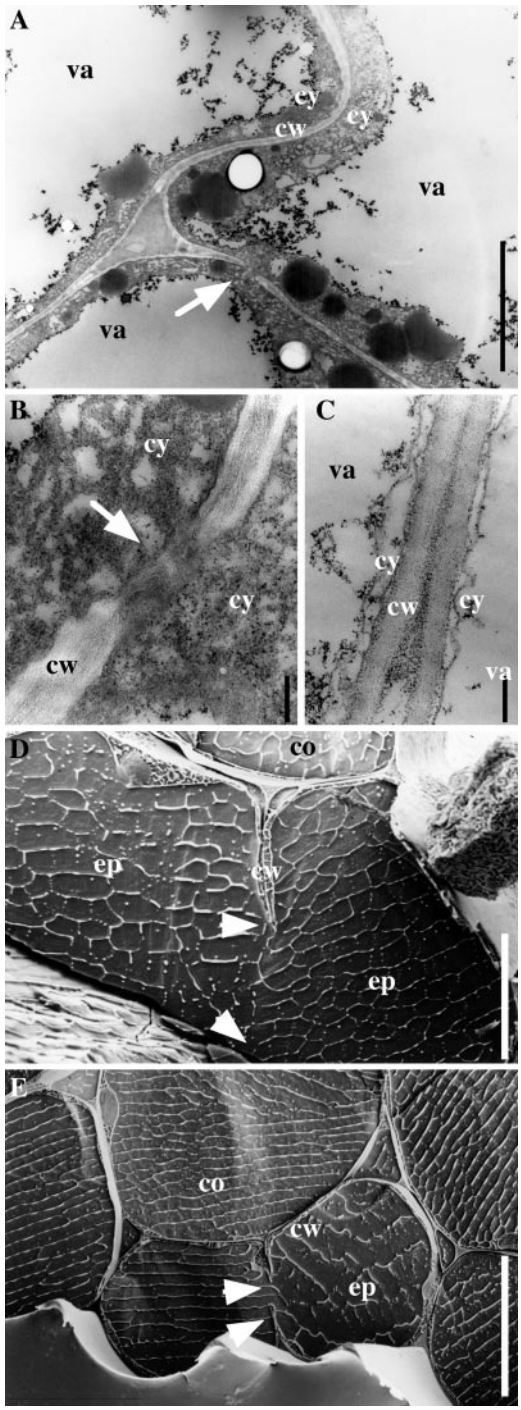

Figure 3. *prc1* Dark-Grown Hypocotyls Display Abnormal Cell Wall Structures.

(A) to **(C)** Transmission electron micrographs of cross-sections from dark-grown hypocotyls (4 days old) of *prc1-1* mutant (**[A]** and **[B]**) and wild-type **(C)** seedlings in the cortical cell layer. Arrow in **(A)** indicates an abnormal wall portion shown at a higher magnification in **(B)**.

(D) and **(E)** Scanning electron micrographs of *prc1-1* dark-grown hypocotyls. Arrowheads indicate protruding stubs of incomplete cell walls in the epidermal cell layer.

co, cortex cell; cw, cell wall; cy, cytoplasm; ep, epidermal cell; va, vacuole. Bar in **(A)** = 1 μm; bars in **(B)** and **(C)** = 0.2 μm; bar in **(D)** = 10 μm; bar in **(E)** = 20 μm.

The inhibition of cellulose by the cellulose synthesis inhibitor DCB in Arabidopsis seedlings causes an accumulation of callose (Nickle and Meinke, 1998). Callose accumulation was also observed in embryos of the cytokinesis-defective mutant *cyt1* (Nickle and Meinke, 1998). We investigated whether also in *prc1* the cellulose deficiency was accompanied by increased callose production. Staining hypocotyl sections as well as permeabilized seedlings with aniline blue or its fluorescent derivative (Stone et al., 1984) revealed a slight accumulation of callose in DCB-treated seedlings. In *prc1-1* hypocotyl sections, we occasionally observed a weak staining, however much weaker than that observed in *cyt1* (data not shown).

Map-Based Cloning of *PRC1*

The *prc1-1* mutation was mapped previously to the bottom of chromosome 5, 1.7 centimorgans (cM) distal to marker m211, in a small mapping population (Desnos, 1996; Desnos et al., 1996). New mapping populations were established by using a cross between *prc1-1* and Landsberg *erecta* (L*er*) as well as by crossing *prc1-1* to a line (in the C24 ecotype) carrying a T-DNA insertion close to the LFY3 restriction fragment length polymorphism marker (Lister and Dean, 1993; Van Lijsebettens et al., 1996). By use of restriction fragment length polymorphism and cleaved amplified polymorphic sequence (Konieczny and Ausubel, 1993) markers, the *prc1-1* mutation was mapped to a region of ~120 kb covered by P1 clones (Liu et al., 1995b) MVP7 and MXK3. As shown in Figure 6A, *prc1-1* is positioned 0.1 cM distal to MUB3.p2B and 1 cM proximal to 4B2-L/2F2-E12.

From the genomic sequence of the 120-kb region containing the *prc1-1* mutation, seven candidate genes were selected. Polymerase chain reaction products for each of these genes were amplified from genomic DNA isolated from several *prc1* alleles, sequenced, and compared with the relevant wild-type sequences. Six *prc1* alleles showed nucleotide substitutions in the sequence of a predicted gene between positions 18,535 and 23,313 on P1 clone MVP7 (GenBank accession number AB025637). All six mutations caused premature stop codons in the predicted coding region. Interestingly, despite their provenance from independent M2 families, *prc1-1* and *prc1-3* showed mutations at identical positions, as did *prc1-4* and *prc1-5*, albeit at a different location (Figure 6). The allele *prc1-19* generated by T-DNA mutagenesis contained a 28-bp deletion

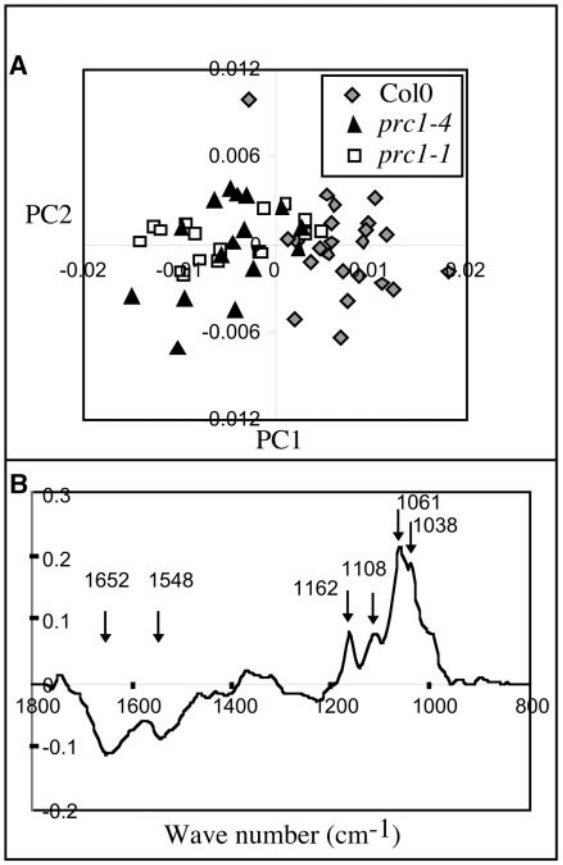

Figure 4. *prc1* Dark-Grown Hypocotyl Cell Walls Are Cellulose Deficient.

(A) FTIR analysis of 4-day-old dark-grown hypocotyls. PC analysis was performed by using 20 FTIR spectra from wild-type and two different *prc1* alleles. PC1 explained 72% of the variance between spectra from wild-type alleles and spectra from *prc1* alleles. Col0, Columbia.

(B) The PC1 loading showed positive peaks characteristic of cellulose in the fingerprint region (1162, 1108, 1061, and 1038 cm^{-1}, respectively), indicating that *prc1* dark-grown hypocotyls were deficient in cellulose relative to the wild type. Two other major peaks (1652, and 1548 cm^{-1}, respectively) appeared negatively in this PC-loading. These peaks corresponded to amide groups of protein, suggesting an enrichment for protein in *prc1* walls relative to the wild type.

(Figure 6), which may be a hallmark of an aborted T-DNA integration.

Isoform of the Cellulose Synthase Family Encoded by *PRC1*

The genomic sequence of *PRC1* perfectly matches five expressed sequence tag (EST) sequences and a previously reported slightly truncated cDNA (*AraxCelA*; GenBank accession number AF062485) (Wu et al., 1998). The gene contains 13 exons and encodes a protein of 1084 amino acids with a predicted molecular mass of 123 kD. PRC1 is a member of a large, ancient family of β-glycosyl transferases present in bacteria, plants, and animals. In higher plants, a subfamily of highly conserved proteins can be distinguished, two members of which (RSW1 and IRX3) have been shown to be essential for cellulose synthesis in Arabidopsis. This subfamily, referred to as *CesA*, probably corresponds to the family of catalytic subunits of cellulose synthase and has at least 10 members in Arabidopsis. According to the classification proposed by Delmer (1999) (see also http://www-plb.ucdavis.edu/labs/delmer/genes.html), *PRC1* corresponds to *CesA6*. The predicted protein structure is shown in Figure 6B.

The PRC1 protein contains the U1, U2, U3, and U4 domains that are characteristic of all β-glycosyl transferases and that form the catalytic domain. A protein fragment of a cotton homolog (CelA1) containing these motifs was shown to bind UDP-glucose in the absence of calcium ions (Kawagoe and Delmer, 1997; Delmer, 1999). All CesA family members from plants contain the so-called plant conserved region and a region that is hypervariable (HVR) between family members. Allele *prc1-9* is predicted to produce a protein truncated at the N-terminus of the first transmembrane domain. In the other mutants analyzed, the predicted truncated product contains only the first two transmembrane domains and part of the catalytic domain. All mutants investigated therefore are expected to be null alleles.

Two CesA Isoforms Required for Normal Cell Expansion in Roots and Dark-Grown Hypocotyl Cells

An intriguing observation is that two mutations in members of the same gene family caused very similar phenotypes in the same cell types. Indeed, the leaky allele *rsw1-10* (H. Höfte, unpublished data) and the null allele *prc1-8* both showed comparable decreases in the length of dark-grown hypocotyls, accompanied by increases in width (Figure 7) in both epidermal and cortical cells (data not shown). FTIR microspectroscopy also indicated a cellulose deficiency in epidermal or cortical cells (or both) in both mutants (Figure 4 and data not shown). The *rsw1-10* mutation was additive to *prc1-8*, as shown by the further shortened hypocotyl length of the double mutant (Figure 7).

One explanation for these observations is that both gene products have comparable functions and contribute to a pool of enzymes that becomes limiting in a mutant background for one or the other locus. However, that situation is unlikely because both mutations are recessive and no striking phenotype was observed in plants that are transheterozygous for both mutations, whereas if the hypothesis described above were true, then the phenotype should be equivalent to that of a single homozygote. In addition, as

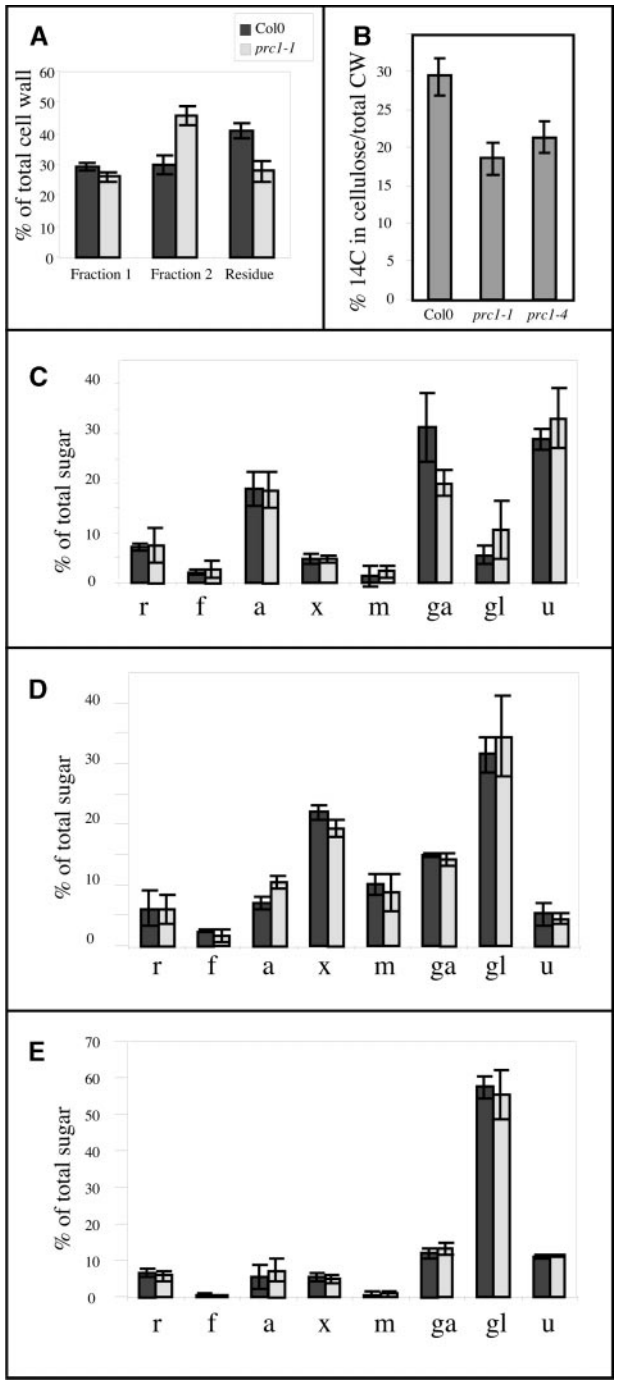

Figure 5. Chemical Analysis Confirms Cellulose Deficiency in Dark-Grown *prc1* Seedlings.

(A) Walls were purified and extracted successively with 0.1 M KOH, yielding a pectin-rich fraction (fraction 1), and 4 M KOH, yielding a hemicellulose-rich fraction (fraction 2). The residual fraction was enriched for a glucan corresponding to cellulose (see text). *prc1-1* walls were deficient for the residual fraction relative to the wild type, indicating a deficiency in cellulose for this mutant. Col0, Columbia.

(B) Incorporation of ^{14}C-glucose (14C) in the acid-resistant cellulosic fraction in wild-type and *prc1* alleles. Each value represents the mean of five independent measurements. CW, cell wall.
(C) to **(E)** Sugar composition of fraction 1 **(C)**, fraction 2 **(D)**, and the residue **(E)**. Only fraction 1 reproducibly showed qualitative differences in sugar composition. r, rhamnose; f, fucose; a, arabinose; x, xylose; m, mannose; ga, galactose; gl, glucose; u, uronic acid.
Error bars indicate ±SD.

shown in Figure 8, even for *prc1-8* segregating in a homozygous *rsw1-10* mutant background, no gene dosage effects were observed, as shown by the strict 1:3 segregation of the additive phenotype. Therefore, even in a situation in which the *RSW1* gene product is growth-limiting, both gene copies of *PRC1*, rather than a single copy, need to be inactivated to result in a further reduction of hypocotyl length. This strongly suggests that the presence of each protein is critical for normal hypocotyl elongation, rather than the size of the combined pool of the CesA1 and CesA6 proteins.

Functional Specialization within the CesA Family

The strong mutant phenotypes for *IRX3* (*CesA7*), *RSW1* (*CesA1*), and *PRC1* (*CesA6*) indicate that the other family members cannot compensate for the absence of their respective gene products. In some cases, this may be simply a result of cell type–specific expression patterns. However, as shown above, this does not seem to be the case, at least not for *RSW1* and *PRC1*. Alternatively, the sequences of different family members may have diverged as adaptations to their specialized cellular roles. To reveal such specialized functions, we investigated the evolutionary relationships between different family members in Arabidopsis and cotton, a species for which a large number of *CesA* ESTs are available in public databases. The sequences of 10 Arabidopsis *CesA* family members were compared with those of three full-length cotton cDNAs and two genes identified by ESTs from different cotton libraries. Because the cotton ESTs corresponded to single-pass sequences close to the 3′ end of the mRNA, we chose the amino acid sequence corresponding to the HVR, which is localized between amino acids 690 and 743 close to the C-terminus of PRC1, to construct a similarity tree. The use of this hypervariable protein segment also maximized the chances to distinguish among the different family members, which in many cases are extremely conserved. A sixth, more divergent, cotton sequence (Gh EST-AI727450), presumably corresponding to a cellulose synthase–like gene (http://cellwall.stanford.edu/cellwall), was used as an outlier in the bootstrap procedure. As shown in Figure 9, amino acid sequences from the five cotton genes did not cluster together but in each case clustered with one or more genes from Arabidopsis. This suggests that the

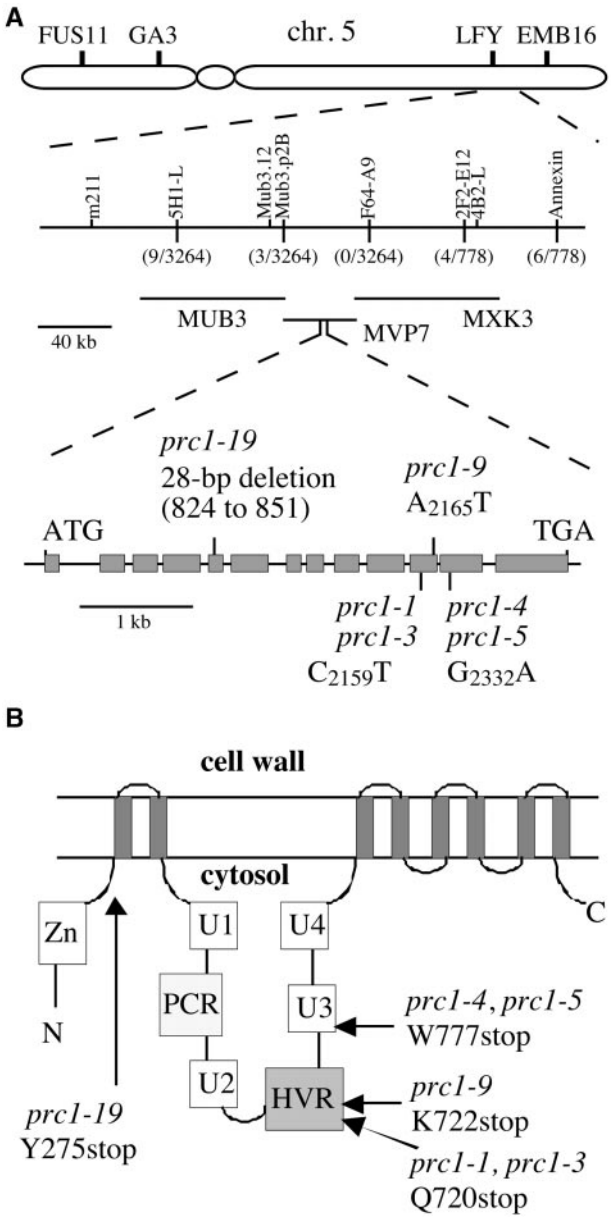

Figure 6. The *PRC1* Gene Is Isolated Through Map-Based Cloning.

(A) Physical map of the region of chromosome (chr.) 5 containing the *PRC1* gene. The *prc1-1* mutation was mapped to the bottom of chromosome 5, south of molecular marker LFY. New markers positioned the *prc1-1* mutation between markers Mub3.p2B and 2F2-E12. The number of recombinant chromosomes is indicated in parentheses. Sequence analysis of candidate genes between these two markers showed that six *prc1* mutant alleles carried a point mutation or a deletion in the *CesA6* gene carried by P1 clone MVP7. The *PRC1* (*CesA6*) gene comprises 13 exons (filled boxes) and 12 introns. The *prc1* mutations that were identified are indicated.

(B) Predicted topology of the PRC1 protein. The protein is predicted to contain eight membrane-spanning helices (indicated by the eight gray bars). The putative Zn binding domain, the U1, U2, U3, and U4 domains, the plant conserved region (PCR), and the HVR are predicted to face the cytosol (Delmer, 1999). The positions of the mutations are indicated. N, N terminus; C, C terminus.

HVR is hypervariable among different family members within a species but is conserved between the orthologs in different species. A very similar tree was obtained when we used the complete amino acid sequences of the Arabidopsis genes and the three full-length cotton genes (data not shown). In conclusion, the divergence between the family members, at least those represented by the five cotton ESTs, must have predated the divergence between Brassicaceae and Malvaceae. Interestingly, *RSW1* and *PRC1* also had their respective orthologs in cotton.

Expression Patterns of *PRC1* and *RSW1* mRNAs

RNA gel blot assays were performed with probes specific for sequences corresponding to a variable region in the respective N termini of *PRC1* and *RSW1* (Figure 10). Both *PRC1* and *RSW1* mRNA were detected in all organs investigated, except in mature flowers. Although the transcript abundance of *PRC1* was less than that of *RSW1*, both mRNAs showed similar expression patterns. In developing seedlings, *RSW1* and *PRC1* mRNAs were high initially and decreased at later growth stages. Expression was high in elongating stems but dropped in the stem sections in which secondary wall synthesis takes place. Interestingly, despite the light-dependent hypocotyl phenotype of *prc1*, we did not obtain evidence for a regulation of *PRC1* at the transcript level: indeed, transcript quantities did not differ between 4-day-old dark-grown and light-grown seedlings.

Similar results were obtained by comparing distributions of the EST sequences corresponding to *RSW1* and *PRC1* obtained from tissue-specific EST libraries (http://cellwall.stanford.edu/cellwall). For instance, in four EST libraries separately covering etiolated seedlings, above-ground tissues, roots, and siliques, we found, respectively, 1, 5, 5, and 1 EST for *PRC1* and 4, 13, 18, and 2 ESTs for *RSW1*. This confirms that *PRC1* expresses fewer transcripts than *RSW1*, that the tissue distribution of each is similar, and that *PRC1* mRNA is present in both dark-grown and light-grown tissues.

DISCUSSION

In this report, we describe the cloning of a novel cellulose synthase required for cell elongation in roots and dark-grown hypocotyls in Arabidopsis. A role for PRC1 (CesA6) in the synthesis of cellulose was supported by two main ob-

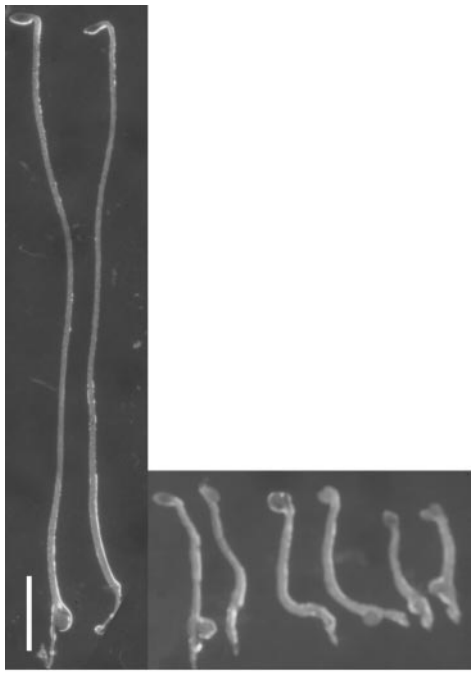

Figure 7. *prc1-8* and *rsw1-10* Have Similar, and Additive, Hypocotyl Phenotypes.

Seedlings were grown for 4 days in the dark. Left to right: wild type (wt), *prc1-8*, *rsw1-10*, and double mutant. The *prc1-8* and *rsw1-10* mutants showed a similar decrease in hypocotyl length compared with wild-type seedlings, whereas the double mutant showed an even shorter hypocotyl. Bar = 2 cm.

servations: *prc1* mutants display a cellulose deficiency, and the *PRC1* gene is a member of the cellulose synthase catalytic subunit family.

Prc1 Phenotype a Result of Cellulose Deficiency

Chemical analysis of the wall composition confirmed a cellulose deficiency in mutant dark-grown seedlings. Indeed, after successive extractions with 0.1 and 4 M KOH, the residual fraction in *prc1-1* was reproducibly 25% less than in wild-type seedlings. This is probably an underestimate, because not all cell types of the dark-grown seedlings were affected by the mutation. This residual fraction was highly enriched for glucose, which in theory could indicate an enrichment for (1→3)-β-glucan (callose), (1→4)-α-glucan (starch), or (1→4)-β-glucan (cellulose). Specific staining with aniline blue failed to detect a substantial accumulation of callose in wild-type or mutant hypocotyl cells. The resistance to strong alkali and the absence of iodine staining also ruled out the presence of starch in this fraction. The residue therefore must consist primarily of cellulose. This was further confirmed by labeling experiments, which showed that less ^{14}C-glucose was incorporated into the nitric/acetic acid–resistant fraction in *prc1* than in the wild type.

A cellulose deficiency was also detected by FTIR microspectroscopy. The advantage of this technique is that the cell wall composition can be assessed at a microscopic level in one or a few cells, whereas chemical methods unavoidably provide an average view of many different cell types. PC analysis of absorption spectra obtained from an area corresponding exclusively to epidermal and cortical cells of dark-grown hypocotyls revealed a cellulose deficiency in mutant cell walls. Similar results were obtained when dark-grown hypocotyls of wild-type seedlings treated with cellulose synthesis inhibitors such as DCB or isoxaben were compared with those of untreated controls, confirming the validity of the method (Fagard, 1999).

PRC1 a Member of the Cellulose Synthase Family

All six mutant alleles sequenced contained premature stop codons in *CesA6*, which in each case removed a major part or even all of the catalytic domain. The *prc1* phenotype is therefore caused by null alleles of the *CesA6* gene. This gene belongs to family 2 of glycosyl transferase, which also contains bacterial cellulose synthases. Previous mutant analysis has shown that at least two other family members, *CesA1* (Arioli et al., 1998) and *CesA7* (Taylor et al., 1999), are required for normal cellulose synthesis in Arabidopsis. Also, the disappearance of rosettes from scanning electron microscopy images of freeze-fractured plasma membranes at the restrictive temperature in *rsw1* (mutant for *CesA1*) and the immunolabeling of *V. angularis* rosettes with antibodies raised against a CesA family member provide strong evidence for a role of these genes in the synthesis of cellulose. A recent study with virus-induced gene silencing in *Nicotiana benthamiana* also showed that the silencing of one or several members of the *CesA* family specifically led to cellulose deficiencies (Burton et al., 2000). The final proof will consist of the in vitro demonstration of cellulose synthesis activity for products of the *CesA* gene family. In the absence of an in vitro assay, the sequence similarity and the cellulose deficiency of *prc1* mutants provide strong evidence that *CesA6* encodes another cellulose synthase catalytic subunit.

Other Cell Wall Changes in *prc1* Mutants

Not only did chemical analysis reveal a deficiency in cellulose, but also mutant walls showed a 50% increase in the hemicellulose-enriched fraction, the composition of which did not differ between wild-type and mutant plants. Only a slight decrease, if any, was observed for the pectin-enriched

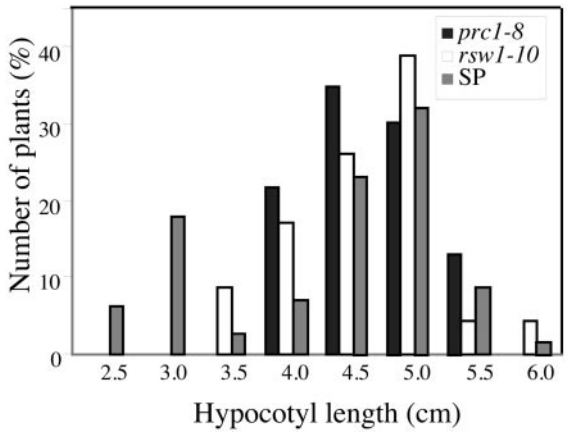

Figure 8. No Gene Dosage Effect Is Observed for *CesA1* and *CesA6*.

Hypocotyl lengths of dark-grown *prc1-8* seedlings, mutant for *CesA6*, *rsw1-10* seedlings, mutant for *CesA1*, and the progeny of a plant homozygous for *rsw1-10* and heterozygous for *prc1-8* were measured. In the segregating population (SP), a discrete 1:3 segregation of the additive phenotype was observed. No gene dosage effect was observed. Indeed, an intermediate hypocotyl length for half of the seedlings, those corresponding to *prc1-8* heterozygotes, would be expected if the dosage of the *CesA6* gene were critical for hypocotyl growth.

fraction. Interestingly, in *prc1-1*, this fraction showed a decreased galactose content without alterations in the content of uronic acid or other sugars. In primary walls, galactose is found mainly on galactan side chains of RG1 and on the side chains of arabinogalactan proteins. However, given the unaltered arabinose content, the simplest explanation is that the cellulose deficiency in *prc1* caused compensatory changes in pectin composition, that is, a decrease in the number or length of the galactan side chains of RG1. We observed similar changes in cell walls of *kor*, another cellulose-deficient mutant (I. His, A. Driouch, F. Goubet, and H. Höfte, unpublished data). The molecular mechanisms underlying these secondary changes and their functional significance, if any, remain to be determined. Finally, the chemical analysis did not provide evidence for the accumulation of substantial amounts of alkali-extractable nonhemicellulosic glucan in *prc1*, whereas such accumulation was reported for *rsw1*.

An intriguing observation was the presence of gapped walls in endodermal, cortical, and epidermal cells of *prc1* hypocotyls and roots. This is unlikely to be an artifact of the sample preparation, because the same defect was observed when using three different sample preparation procedures, including scanning electron microscopy, which does not involve tissue fixation. This defect is reminiscent of the stubs observed in cytokinesis mutants. Cortical and epidermal hypocotyl cells essentially have an embryonic origin, and no additional postembryonic divisions take place, except for those that contribute to the formation of stomatal guard cells. Because no gapped walls were observed in immature or mature embryos or in light-grown hypocotyls, the defect must arise during cell expansion. The simplest explanation would be that radial walls, the architecture of which is not compatible with wall expansion, rupture as a result of the increased radial expansion caused by the cellulose deficiency. That would be unlikely, however, because several other radial expansion mutants did not show gapped walls (Nicol et al., 1998; Bichet et al., 2001). An alternative explanation is that wall expansion, presumably mediated by

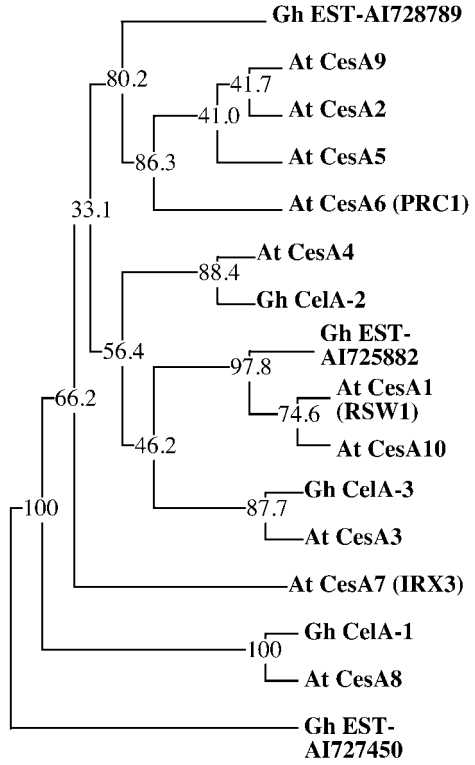

Figure 9. Members of the *CesA* Family Exhibit Functional Specialization.

Shown is a phylogenetic tree based on the HVR (see text and Figure 5) of protein sequences of Arabidopsis and cotton *CesA* family members. Alignment data are from bootstrap values sampled 100 times and used to construct the consensus tree shown. Numbers are bootstrap values and indicate the number of trees in which the proteins to the right of the bootstrap values clustered together. Gh EST-AI727450 was included as an outlier. The five other cotton genes did not cluster together but instead clustered with one or two Arabidopsis sequences, suggesting that the CesA amino acid sequences diverged before the divergence between Brassicaceae and Malvaceae; that, in turn, suggests a functional specialization of most CesA isoforms.

At, *Arabidopsis thaliana*; Gh, *Gossypium hirsutum*.

wall-loosening proteins such as expansins, continues in the absence of sufficient cellulose synthesis to maintain a constant wall thickness. This eventually may lead to the rupture of the walls. Interestingly, the space between the wall stubs often contained wall material, composed of at least xyloglucan and pectin, as found with specific antibodies (data not shown). These results suggest that at least in mutant walls, impaired cellulose synthesis does not feed back to the wall-loosening machinery and the synthesis of other wall polysaccharides.

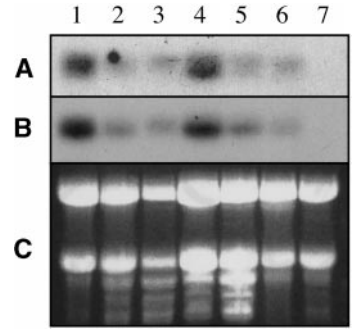

Figure 10. *PRC1* and *RSW1* Have Similar Transcript Profiles.

Total RNA of different samples was hybridized with labeled probes corresponding to a variable sequence at the N-terminal end of CesA proteins.
(A) *PRC1* probe.
(B) *RSW1* probe.
(C) Ethidium bromide–stained agarose gel of the same samples.
Lane 1, 1-day-old germinating seeds; lane 2, 4-day-old dark-grown seedlings; lane 3, 4-day-old light-grown seedlings; lane 4, elongating inflorescence stem sections; lane 5, mature leaves; lane 6, roots; lane 7, mature flowers.

Functional Specialization within the Cellulose Synthase Gene Family

Large gene families are more the rule than the exception in plants, including Arabidopsis. Reverse genetics frequently has failed to associate clear-cut mutant phenotypes with mutations in individual genes within such families (Gilliland et al., 1998; D. Bouchez, personal communication). This suggests that many gene family members may have at least partially redundant roles. The *CesA* gene family is atypical in this respect, in that strong mutant phenotypes have been observed for at least three genes. Tissue-specific expression may explain specific phenotypes in some cases, for example, *RSW1* in cells producing primary walls and *IRX3* in xylem elements producing secondary walls. However, the conservation of specific amino acid sequence motifs, such as the HVR, between species suggests a functional specialization of different isoforms. We think it likely that the HVR domain interacts with other proteins with specific roles in different cell types or environmental conditions.

Another complication involves the observation that in some cell types at least two isoforms are required for normal cellulose synthesis. Indeed, *rsw1-1* is affected in all cell types at the restrictive temperature, including in cells in the hypocotyl and root (Arioli et al., 1998). Cell expansion defects in all expanding cell types, including those in the central cylinder, were also observed in roots and hypocotyls of *rsw1-10*. The phenotype of *rsw1-10* is less severe than *rsw1-1* at the restrictive temperature (data not shown), which suggests that *rsw1-10* is a leaky allele. Null alleles of *PRC1* also showed expansion defects in endodermis, cortex, and epidermis of dark-grown hypocotyls and roots, indicating a requirement for both gene products to support normal cellulose synthesis and cell expansion in these cell types. The simplest explanation for this observation is a quantitative one: to sustain the demand for cellulose in the cell, a sufficiently large pool of CesA protein is required, which in turn requires synthesis from both genes. The strictly recessive phenotypes for both genes do not support a strong dependence on dose. An even stronger argument against this hypothesis is the absence of a gene dosage effect in a population segregating for the *prc1-8* mutation in a genetic background homozygous for *rsw1-10*. The results suggest a strict requirement for two distinct isoforms rather than a certain pool size of CesA protein. This implies that different CesA isoforms need to be present at different times in the same cell or at different locations within the cell. Alternatively, CesA isoforms may act in concert or might form heterodimers. Immunolocalization studies with specific antibodies or with epitope-tagged versions of RSW1 (CesA1) and PRC1 (CesA6) should clarify this issue.

A final intriguing observation is the light-dependent conditional phenotype in mutant *prc1* hypocotyls. We previously showed that the rescue of the hypocotyl phenotype is mediated by phytochrome (Desnos et al., 1996). The simplest explanation for this phenomenon is that phytochrome controls the expression of one or more other *CesA* isoforms, which either replace *PRC1* (*CesA6*) in light-grown hypocotyls or have a function redundant with it. These observations indicate that phytochrome acts on the cellulose synthesis machinery and suggest a connection between phytochrome signaling and cell wall–related processes involved in growth control. RNA gel blot experiments thus far do not provide evidence for the regulation of *PRC1* mRNA quantities by light. We are currently investigating the control by phytochrome of the expression of other *CesA* family members.

METHODS

Plant Material and Growth Conditions

Wild-type *Arabidopsis thaliana* plants were of the Columbia (Col-0), Wassilewskija (Ws), or Landsberg *erecta* (L*er*) ecotype. Alleles *prc1-1*

through *prc1-4* have been described previously (Desnos et al., 1996) and were of the Col-0 ecotype; these lines were all backcrossed four times. Alleles *prc1-5* through *prc1-7*, *prc1- 9*, and *prc1-11* (T. Desnos, F. Nicol, and H. Höfte, unpublished data; P. Benfey and M.-T. Hauser, personal communication) were of the Col-0 ecotype; these lines were backcrossed two, two, one, two, and one time, respectively. Mutant *rsw1-1* was of the Col-0 ecotype (Arioli et al., 1998). Mutants *rsw1-10*, *prc1-8*, *prc1-10*, *prc1-12*, and *prc1-19* were isolated from T-DNA–mutagenized populations and were of the Ws ecotype.

For growth in vitro, plants were grown on Petri dishes containing Murashige and Skoog (1962) medium (Estelle and Somerville, 1987) without sucrose at 25°C. For dark growth, seeds were cold-treated for 48 hr and then exposed to fluorescent white light (200 $\mu M.m^{-2}.sec^{-1}$) for 2 hr to synchronize germination, and finally the plates were wrapped in three layers of aluminum foil. For culture in the light, seeds were cold-treated for 48 hr and then placed under fluorescent white light (200 $\mu M.m^{-2}.sec^{-1}$) in 16-hr-light/8-hr-dark cycles. The time of measurement or collection of tissue was counted as days after the beginning of the light treatment. For cellulose incorporation assays, 200 Arabidopsis seedlings were grown at 20°C in the dark for 3 days in 10 mL of liquid medium containing 0.5% glucose. Seeds were cold-treated for 48 hr and then exposed to fluorescent white light (200 $\mu M.m^{-2}.sec^{-1}$) for 5 hr to synchronize germination, after which the flasks were wrapped in three layers of aluminum foil.

Measurement of Hypocotyl and Root Lengths

The growth of the seedlings was arrested by adding an aqueous solution of 0.4% formaldehyde. Hypocotyls and roots were spread on agar plates, and their image was captured with a digital camera. Lengths were measured by using image analysis software (Optimas 5.2; IMASYS, Surennes, France), as described by Gendreau et al. (1997).

Cross-Sections

For light microscopy, seedlings were fixed in PBS buffer containing 4% paraformaldehyde and 0.2% glutaraldehyde and were embedded in historesin (Technovit 7100; Kulzer, Wehrheim, Germany), according to the manufacturer's instructions. Sections 3 μm thick were cut by using a Jung RM2055 microtome (Leica Instruments, Nussloch, Germany). The cross-sections were stained with a 0.005% aqueous solution of Calcofluor (fluorescent brightener 28; Sigma) for 2 min and visualized under UV light with a Microphot FXA microscope (Nikon, Champigny-sur-Marne, France).

For transmission electron microscopy, seedlings were fixed with a 2.5% glutaraldehyde solution in phosphate buffer and then stained with a 2% osmium tetroxide solution. Seedlings were then embedded in Epon resin (TAAB 812, TAAB Laboratories Equipment Ltd., Reading, UK). Ultrathin sections (100 nm thick) were cut with a Reichert (Leica Instruments) Ultracut E ultramicrotome and deposited on 300-mesh copper–palladium grids. Samples were stained a second time with a 5% uranyl acetate solution followed by a 0.5% lead citrate solution and visualized with an EM 420 transmission electron microscope (Philips, Eindhoven, The Netherlands) at 80-kV acceleration.

Fourier Transform Infrared Spectroscopy

The seedlings (10 for each condition) were pressed onto a barium fluoride window and rinsed with water to remove cytoplasmic debris. The samples were dried at 37°C for 20 min. Two spectra of each seedling were collected on a Bio-Rad FTS-40 FT spectrometer in the middle region of the hypocotyl, avoiding the central cylinder, in a 60- $\times$ 40-μm window. Because absorbance varies with sample thickness, all data sets were corrected for baseline and normalized for area before statistical methods were applied. Exploratory principal components analysis was performed with Win-Discrim software (E.K. Kemsley, Institute of Food Research, Norwich, UK). Reference infrared absorption spectra of cellulose and other β-glucans were obtained from the literature (Tsuboi, 1957; Liang and Marchessault, 1959; Séné et al., 1994).

Preparation of Cell Wall Material

The plants were incubated for 30 min in 90% ethanol at 65°C to inactivate enzymes. The tissues were then ground in a Tenbroeck glass Potter–Elvehjem homogenizer (Janke and Kunkel IKA Labortechnik, Staufen, Germany). The homogenate was centrifuged at 2300*g* for 15 min. The pellet was washed with ethanol (three or four times), methanol/chloroform (2:3 [v/v], overnight), and ethanol again. The remaining pellet, which contained the cell wall, was dried overnight at 80°C. The yield of cell walls was defined as the weight (in grams) of dry cell walls per 100 g of fresh plants.

Extraction of Polymers

Pectic and hemicellulosic polymers were solubilized successively from cell walls by treatments with 0.1 M KOH at 20°C (three times for 1 hr) and 4 M KOH at 20°C (three times for 1 hr), respectively. The remaining pellet was washed with water until the pH of the supernatant was equal to that of water. The KOH extracts were neutralized with HCl, dialyzed against water with a molecular weight cutoff of 1000, and lyophilized.

Sugar Composition

Neutral sugar composition was determined as described by Englyst and Cummings (1984). Inositol was added to samples as an internal reference. Uronic acid contents were determined as described by Thibault (1979).

Cellulose Incorporation Assays

Two hundred Arabidopsis seedlings, grown in liquid culture in the dark, as described above, were washed three times with 15 mL of glucose-free growth medium before being resuspended in 1 mL of growth media containing ^{14}C-glucose (NEN Research, Boston, MA), 1.0 $\mu Ci.mL^{-1}$. The seedlings were then incubated for 1 hr in the dark at 15°C in glass tubes. After treatment, the seedlings were washed three times with 6 mL of glucose-free growth medium and then extracted with 5 mL of boiling absolute ethanol for 20 min. This step was repeated three times. Next, seedlings were resuspended in 3 mL of chloroform/methanol (1:1 [v/v]), extracted for 20 min at 45°C, and finally resuspended in 3 mL of acetone for 15 min at room temperature with gentle shaking. The remaining material was resuspended in 500 μL of an acetic acid/nitric acid/water solution (8:1:2 [v/v/v]), as described by Updegraff (1969), for 1 hr in a boiling water bath. Acid-soluble material and acid-insoluble material were separated by vacuum filtration through glass microfiber filters (GF/A; 2.5 cm diameter;

Whatman, Maidstone, UK), after which the filters were washed with 1.5 mL of water. The acid solution and water wash constitute the acid-soluble fraction. Finally, the filters were washed with 30 mL of water and 20 mL of ethanol, yielding the acid-insoluble fraction, which is essentially crystalline cellulose. The amount of label in each fraction was determined by scintillation counting in a Betamatic scintillation counter (Kontron Instruments, Montigny le Bretonneux, France) using Ultima-Flo AP (Packard, Groningen, The Netherlands) as the scintillation liquid. The percentage of label incorporation was expressed as 100 × the ratio between the amount of label in the cellulosic fraction and the amount in the acid-soluble plus cellulosic fractions.

Genetic Analysis and Map-Based Cloning

The *prc1-1* mutant (ecotype Col-0; backcrossed three times to Col-0) was crossed to line KanR5 (ecotype C24), which bears a T-DNA (conferring resistance to kanamycin) inserted close to marker LFY3 (Van Lijsebettens et al., 1996) at the bottom of chromosome 5 (Lister and Dean, 1993). F_2 seedlings were sown on Murashige and Skoog medium supplemented with 50 mM kanamycin and grown for 3 days in total darkness. Of these, 1632 seedlings with short hypocotyls were scored and cultured for 3 more days in white light. Individuals with the *prc1* phenotype and resistant to kanamycin were considered recombinant between the *prc1-1* mutation and the T-DNA insertion. These plants were transferred to the greenhouse, and genomic DNA was extracted from leaves and flower buds, as described previously (Bouchez and Camilleri, 1998).

To determine the position of the *prc1-1* mutation, DNA of the recombinant plants was analyzed with restriction fragment length polymorphism marker 5H1-L; this marker was designed by isolating the left border of yeast artificial chromosome 5H1 using the vectorette technique (Riley et al., 1990) and looking for polymorphism between the Col-0 and C24 ecotypes by DNA gel blotting with different restriction enzymes. The MUB3.12 and MUB3.p2B cleaved amplified polymorphic sequence (CAPS) markers were designed by polymerase chain reaction amplification of introns from genes 12 and p2B of P1 clone MUB3 (GenBank accession number AB010076) and digestion of the polymerase chain reaction products, amplified from genomic DNA of Col-0 and C24 ecotypes, with pools of restriction enzymes (40 were tested in all). The MUB3.12 marker (specific oligonucleotides: forward, CGCCGACGGAGAAATGACCAAG; reverse, TCACCAACACGAATGCGAGTACGA) is polymorphic for an EcoRI restriction site that is present in ecotype Col-0 but absent in C24 and L*er*, whereas the MUB3.p2B marker (specific oligonucleotides: forward, CTCTCCCAAAGTAATCGTGCTA; reverse, TACCAGATGAACAGGGCTAAGT) is polymorphic for an AccI site that is present in C24 but not in Col-0.

The *prc1-1* mutant was also crossed to a wild-type plant of the L*er* ecotype. F_2 seedlings were grown in the dark on Murashige and Skoog medium, and individuals homozygous for the *prc1-1* mutation were selected on the basis of their short hypocotyls. These plants were transferred to the greenhouse, and genomic DNA was extracted from leaves and flower buds (Edwards et al., 1991). Recombinant individuals were identified by using CAPS markers based on partial sequences of markers ATPK41B (Recombinant inbred marker; Lister and Dean, 1993) and ATHB-5 (GenBank accession number X67033). Specific oligonucleotides (forward, TGTGATCAGAAATGGATCG; reverse, CTTCCTGTGTTGCTCTCGTT) amplified an ~700-bp fragment at the ATPK41B locus, which was found, by testing with 40 commonly used restriction enzymes, to be cleaved by HinfI in the L*er* allele but not in the Col-0 allele. For optimal resolution of the polymorphism, the polymerase chain reaction fragments were also cut with the restriction enzyme DraI. Other specific oligonucleotides (forward, TAACCAGCTCATCAACCAAAC; reverse, AAGATGGAAACAGAGAATTGACTA) amplified an ~850-bp fragment at the ATHB-5 locus, which is cleaved by the restriction enzyme AvaI in the Col-0 allele but not in the L*er* allele. Recombinant inbred marker Annexin (ve028; Lister and Dean, 1993) was converted to a CAPS marker (specific oligonucleotides: forward, TCCACCAAGATGTTCACCAAGA; reverse, CGTTCCATGTCAACTTCAGTTC) by using the restriction enzyme TfiI. Finally, a restriction fragment length polymorphism marker (2F2-E12) was found on the proximal part of P1 clone MXK3, which is polymorphic for an HpaII restriction site between L*er* and Col-0.

RNA Gel Blotting

RNAs were extracted as described previously (Brusslan and Tobin, 1992). RNA gel blotting on Hybond N membranes and labeling of the probes by random priming in the presence of 50 μCi of ^{32}P-dCTP was performed according to the manufacturer's instructions (Amersham, Little Chalfont, UK). The membrane was hybridized overnight at 42°C in 10 mL of SDS-rich buffer, as described by Church and Gilbert (1984) with 50% formamide and 100 μg/mL salmon sperm DNA after overnight prehybridization. Washes were performed at 65°C in 2 × SSC (1 × SSC is 0.15 M NaCl and 0.015 M sodium citrate) plus 0.1% SDS for 15 min and again for 15 min in 1 × SSC plus 0.1% SDS (once for the *RSW1* probe and twice for the *PRC1* probe).

The *RSW1* probe was prepared with a 300-bp-long EcoRV-HincII fragment covering the N-terminal variable region, which is specific for each *CesA* (positions 322 to 622 from ATG). The *PRC1* probe was prepared with a 379-bp-long BglII-HindIII fragment covering the same region (positions 237 to 616 from ATG). The specificity of the probes was tested on dot blots of cloned cDNAs corresponding to Arabidopsis cellulose synthase genes, in the same hybridization conditions as those used for the RNA gel blots. The hybridization signal of the *RSW1* probe was at least 10-fold greater for *RSW1* than for *PRC1*. The hybridization signal of the *PRC1* probe was at least 10-fold greater for *PRC1* than for the very similar sequence *CesA5* and at least 100-fold greater than for *RSW1* (data not shown).

Phylogenetic Analysis

Unrooted trees were built by using an alignment of a variable region corresponding to amino acids 690 and 743 in PRC1 obtained with the program ClustalW (http://www.infobiogen.fr/services/analyseq/cgi-bin/clustalw_in.pl). This alignment was used by the algorithm PROTPARS (also available at the above-mentioned website) to construct a consensus tree from 100 bootstrapped data sets.

ACKNOWLEDGMENTS

We thank Brigitte Gelie, Jocelyne Kronenberger, Joël Talbotec, Sigolène Müller, Audrey Hantiu, and Olivier Grandjean for technical assistance; Estelle Aletti for providing the data described in Figure 7; Hervé Vaucheret for enthusiastic discussions and critical reading of

the manuscript; Phillip Benfey and Marie-Therese Hauser for providing *prc* alleles; and Reginald Wilson for insightful advice regarding FTIR. We thank Vincent Chiang for kindly providing the AraxCelA cDNA clone. Jean-François Thibault and Marc Lahaye are thanked for thoughtful advice concerning sugar chemistry and for making their equipment available. The Arabidopsis Biological Resources Center and the Nottingham Stock Centre are thanked for providing seed and DNA stocks. This work was financed in part by Framework 4 Grant PHOTARCH (No. BIO4-CT97-2124) from the European Economic Community; Grant No. A.I.P. 00176 from the Groupement de Recherche, Génomes et Mutants d'Arabidopsis; and Grant No. ACC-SV 9501006 from the Ministère de la Recherche et de la Technologie. T. Desnos and M.F. were bursaries from the Ministère de la Recherche et de la Technologie.

Received June 1, 2000; accepted October 4, 2000.

REFERENCES

Amor, Y., Haigler, C.H., Johnson, S., Wainscott, M., and Delmer, D.P. (1995). A membrane-associated form of sucrose synthase and its potential role in synthesis of cellulose and callose in plants. Proc. Natl. Acad. Sci. USA **92,** 9353–9357.

Arioli, T., Peng, L., Betzner, A.S., Burn, J., Wittke, W., Herth, W., Camilleri, C., Hofte, H., Plazinski, J., Birch, R., Cork, A., Glover, J., Redmond, J., and Williamson, R.E. (1998). Molecular analysis of cellulose biosynthesis in Arabidopsis. Science **279,** 717–720.

Assaad, F.F., Mayer, U., Wanner, G., and Jurgens, G. (1996). The KEULE gene is involved in cytokinesis in Arabidopsis. Mol. Gen. Genet. **253,** 267–277.

Bichet, A., Desnos, T., Turner, S., Grandjean, O., and Höfte, H. (2001). *BOTERO1* is required for normal orientation of cortical microtubules and anisotropic cell expansion in *Arabidopsis*. Plant J., in press.

Bouchez, D., and Camilleri, C. (1998). High molecular weight DNA extraction from Arabidopsis. Methods Mol. Biol. **82,** 61–70.

Brusslan, J.A., and Tobin, E.M. (1992). Light-independent developmental regulation of *CAB* gene expression in *Arabidopsis thaliana* seedlings. Proc. Natl. Acad. Sci. USA **89,** 7791–7795.

Burton, R.A., Gibeat, D.M., Bacic, A., Findlay, K., Roberts, K., Hamilton, A., Baulcombe, D., and Fincher, G.B. (2000). Virus-induced silencing of a plant cellulose synthase gene. Plant Cell **12,** 691–705.

Carpita, N.C., and Gibeaut, D.M. (1993). Structural models of primary cell walls in flowering plants: Consistency of molecular structure with the physical properties of the walls during growth. Plant J. **3,** 1–30.

Church, G.M., and Gilbert, W. (1984). Genomic sequencing. Proc. Natl. Acad. Sci. USA **81,** 1991–1995.

Delmer, D. (1999). Cellulose biosynthesis: Exciting times for a difficult field of study. Annu. Rev. Plant Physiol. Plant Mol. Biol. **50,** 245–276.

Desnos, T. (1996). Etude Génétique et Physiologique de l'Elongation Cellulaire chez *Arabidopsis thaliana*. (Paris: Sciences de la Vie).

Desnos, T., Orbovic, V., Bellini, C., Kronenberger, J., Caboche, M., Traas, J., and Höfte, H. (1996). Procuste1 mutants identify two distinct genetic pathways controlling hypocotyl cell elongation, respectively, in dark- and light-grown Arabidopsis seedlings. Development **122,** 683–693.

Edwards, K., Johnstone, C., and Thompson, C. (1991). A simple and rapid method for the preparation of plant genomic DNA for PCR analysis. Nucleic Acids Res. **19,** 1349.

Emons, A. (1985). Role of particle rosettes and terminal globules in cellulose synthesis. In Biosynthesis and Biodegradation of Cellulose, C. Haigler and P. Weimer, eds (New York: Marcel Dekker), pp. 71–98.

Englyst, H.N., and Cummings, J.H. (1984). Simplified method for the measurement of total non-starch polysaccharides by gas–liquid chromatography of constituent sugars as alditol acetates. Analyst **109,** 937–942.

Estelle, M.A., and Somerville, C. (1987). Auxin-resistant mutants of *Arabidopsis thaliana* with an altered morphology. Mol. Gen. Genet. **206,** 200–206.

Fagard, M. (1999). Analyse Physiologique et Moléculaire du Mutant *procuste1* d'*Arabidopsis thaliana* Affecté dans l'Elongation Cellulaire. (Paris: Sciences de la Vie).

Gendreau, E., Traas, J., Desnos, T., Grandjean, O., Caboche, M., and Höfte, H. (1997). Cellular basis of hypocotyl growth in *Arabidopsis thaliana*. Plant Physiol. **114,** 295–305.

Giddings, T.H., and Staehelin, L.A. (1991). Microtubule-mediated control of microfibril deposition: A re-examination of the hypothesis. In The Cytoskeletal Basis of Plant Growth and Form, C.W. Lloyd, ed (New York: Academic Press), pp. 85–99.

Gilliland, L., McKinney, E., Asmussen, M., and Meagher, R. (1998). Detection of deleterious genotypes in multigenerational studies. I. Disruptions in individual actin genes. Genetics **2,** 717–725.

Green, P.B. (1994). Connecting gene and hormone action to form, pattern and organogenesis: Biophysical transductions. J. Exp. Bot. **45,** 1775–1788.

Hauser, M.T., Morikami, A., and Benfey, P.N. (1995). Conditional root expansion mutants of Arabidopsis. Development **121,** 1237–1252.

Kawagoe, Y., and Delmer, D. (1997). Pathways and genes involved in cellulose biosynthesis. Genet. Eng. **19,** 63–87.

Kemsley, E.K. (1998). Chemometric Methods for Classification Problems: Discriminant Analysis and Modelling of Spectroscopic Data (Chichester, UK: John Wiley & Sons), pp. 1–47.

Kimura, S., Laosinchai, W., Itoh, T., Cui, X., Linder, R., and Brown, R. (1999). Immunogold labeling of rosette terminal cellulose-synthase complexes in the vascular plant *Vigna angularis*. Plant Cell **11,** 2075–2085.

Konieczny, A., and Ausubel, F.M. (1993). A procedure for mapping Arabidopsis mutations using co-dominant ecotype-specific PCR-based markers. Plant J. **4,** 403–410.

Liang, C.Y., and Marchessault, R.H. (1959). Infrared spectra of crystalline polysaccharides. II. Native celluloses in the region from 640 to 1700 cm^{-1}. J. Polym. Sci. **31,** 269–278.

Lister, C., and Dean, C. (1993). Recombinant inbred lines for mapping RFLP and phenotypic markers in *Arabidopsis thaliana*. Plant J. **4,** 745–750.

Liu, C.-M., Johnson, S., and Wang, T.L. (1995a). *cyd*, a mutant of pea that alters embryo morphology, is defective in cytokinesis. Dev. Genet. **16,** 321–331.

Liu, Y.-G., Mitsukawa, N., Vazquez-Tello, A., and Whittier, R.F. (1995b). Generation of a high-quality P1 library of Arabidopsis suitable for chromosome walking. Plant J. **7,** 351–358.

Lukowitz, W., Mayer, U., and Jürgens, G. (1996). Cytokinesis in the Arabidopsis embryo involves the syntaxin-related KNOLLE gene product. Cell **84,** 61–71.

Maeda, H., and Ishida, N. (1967). Specificity of binding of hexopyranosyl polysaccharides with fluorescent brightener. J. Biochem. **62,** 276–278.

Matthysse, A.G., Thomas, D.L., and White, A.R. (1995a). Mechanism of cellulose synthesis in *Agrobacterium tumefaciens*. J. Bacteriol. **177,** 1076–1081.

Matthysse, A.G., White, S., and Lightfoot, R. (1995b). Genes required for cellulose synthesis in *Agrobacterium tumefaciens*. J. Bacteriol. **177,** 1069–1075.

McCann, M.C., and Roberts, K. (1994). Changes in cell wall architecture during cell elongation. J. Exp. Bot. **45,** 1683–1691.

McCann, M., Chen, L., Roberts, K., Kemsley, E.K., Séné, C., Carpita, N.C., Stacey, N.J., and Wilson, R.H. (1997). Infrared microspectroscopy: Sampling heterogeneity in plant cell wall composition and architecture. Physiol. Plant. **100,** 729–738.

Murashige, T., and Skoog, F. (1962). A revised medium for rapid growth and bioassays with tobacco tissue culture. Physiol. Plant. **15,** 473–497.

Nickle, T.C., and Meinke, D.W. (1998). A cytokinesis-defective mutant of Arabidopsis (cyt1) characterized by embryonic lethality, incomplete cell walls, and excessive callose accumulation. Plant J. **15,** 321–332.

Nicol, F., His, I., Jauneau, A., Vernhettes, S., Canut, H., and Höfte, H. (1998). A plasma membrane–bound putative endo-1,4-beta-D-glucanase is required for normal wall assembly and cell elongation in Arabidopsis. EMBO J. **17,** 5563–5576.

Pear, J.R., Kawagoe, Y., Schreckengost, W.E., Delmer, D.P., and Stalker, D.M. (1996). Higher plants contain homologs of the bacterial celA genes encoding the catalytic subunit of cellulose synthase. Proc. Natl. Acad. Sci. USA **93,** 12637–12642.

Peng, L., Hocart, C.H., Redmond, J.W., and Williamson, R.E. (2000). Fractionation of carbohydrates in Arabidopsis root cell walls shows that three radial swelling loci are specifically involved in cellulose production. Planta **211,** 406–414.

Riley, J., Butler, R., Ogilvie, D., Finniear, R., Jenner, D., Powell, S., Anand, R., Smith, J.C., and Markham, A.F. (1990). A novel, rapid method for the isolation of terminal sequences from yeast artificial chromosome (YAC) clones. Nucleic Acids Res. **18,** 2887–2890.

Saxena, I.M., Lin, F.C., and Brown, R.M.J. (1990). Cloning and sequencing of the cellulose synthase catalytic subunit gene of *Acetobacter xylinum*. Plant Mol. Biol. **16,** 673–683.

Séné, C., McCann, M., Wilson, R.H., and Grinter, R. (1994). FT-Raman and FT-infrared spectroscopy: An investigation of five higher plant cell walls and their components. Plant Physiol. **106,** 1623–1633.

Stone, B.A., Evans, N.A., Bonig, I., and Clarcke, A.E. (1984). The application of Sirofluor, a chemically defined fluorochrome from aniline blue, for the histochemical detection of callose. Protoplasma **122,** 191–195.

Taylor, N., Scheible, W., Cutler, S., Somerville, C., and Turner, S. (1999). The irregular xylem3 locus of Arabidopsis encodes a cellulose synthase required for secondary cell wall synthesis. Plant Cell **11,** 769–780.

Thibault, J.-F. (1979). Automatisation du dosage des substances pectiques par la méthode du méta-hydroxyphenyl. Lebensm. Wiss. Technol. **12,** 247–251.

Tsuboi, M. (1957). Infrared spectrum and crystal structure of cellulose. J. Polym. Sci. **25,** 159–171.

Updegraff, D.M. (1969). Semi-micro determination of cellulose in biological materials. Anal. Biochem. **32,** 420–424.

Van Lijsebettens, M., Wang, X., Cnops, G., Boerjan, W., Desnos, T., Höfte, H., and Van Montagu, M. (1996). Transgenic Arabidopsis tester lines with dominant marker genes. Mol. Gen. Genet. **251,** 365–372.

Vian, B., and Reis, D. (1991). Relationship of cellulose and other cell wall components: Supramolecular organisation. In Biosynthesis and Biodegradation of Cellulose, C. Haigler and P. Weimer, eds (New York: Marcel Dekker), pp. 25–50.

Wu, L., Joshi, C.P., and Chiang, V.L. (1998). AraxCelA, a new member of cellulose synthase gene family from *Arabidopsis thaliana* (accession no. AF 062485) (PGR98–114). Plant Physiol. **117,** 1125.

Wymer, C., and Lloyd, C. (1996). Dynamic microtubules: Implications for cell wall patterns. Trends Plant Sci. **1,** 222–228.

Zablackis, E., Huang, J., Müller, B., Darvill, A.G., and Albersheim, P. (1995). Characterization of the cell-wall polysaccharides of *Arabidopsis thaliana* leaves. Plant Physiol. **107,** 1129–1138.

PROCUSTE1 Encodes a Cellulose Synthase Required for Normal Cell Elongation Specifically in Roots and Dark-Grown Hypocotyls of Arabidopsis

Mathilde Fagard, Thierry Desnos, Thierry Desprez, Florence Goubet, Guislaine Refregier, Gregory Mouille, Maureen McCann, Catherine Rayon, Samantha Vernhettes and Herman Höfte

Plant Cell 2000;12;2409-2423
DOI 10.1105/tpc.12.12.2409